

Probes for measuring fluctuation-induced Maxwell and Reynolds stresses in the edge of the Madison Symmetric Torus reversed field pinch^{a)}

A. Kuritsyn,^{b)} G. Fiksel, M. C. Miller, A. F. Almagri, M. Reyfman, and J. S. Sarff

Center for Magnetic Self-Organization in Laboratory and Astrophysical Plasmas and Department of Physics, University of Wisconsin-Madison, Madison, Wisconsin 53706, USA

(Presented 14 May 2008; received 9 May 2008; accepted 9 June 2008; published online 31 October 2008)

Several probes have been constructed to measure fluctuation-induced Maxwell and Reynolds stresses in the edge of the Madison Symmetric Torus reversed field pinch (RFP). The magnetic probe is composed of six magnetic pickup coil triplets. The triplets are separated spatially, which allows for local measurements of the Maxwell stress. To measure the plasma flow components for evaluation of the Reynolds stress, we employ a combination of an optical probe [Kuritsyn *et al.*, Rev. Sci. Instrum. **77**, 10F112 (2006)] and a Mach probe. The optical probe measures the radial ion flow locally using Doppler spectroscopy. The Mach probe consists of four current collectors biased negatively with respect to a reference tip and allows for measurements of the poloidal and toroidal components of the bulk plasma flow. The stresses are observed to play an important role in the momentum balance in the RFP edge during internal reconnection events. © 2008 American Institute of Physics. [DOI: 10.1063/1.2955930]

I. INTRODUCTION

Plasma rotation plays a central role in the formation of internal transport barriers, the transition to high-confinement H mode,¹ and in the stabilization of resistive wall modes² in toroidal magnetic configurations. Thus, it is important to understand the underlying physics of flow generation and transport.

The reversed field pinch (RFP) is a toroidal plasma configuration similar to a tokamak but with a relatively weak toroidal magnetic field that reverses its sign near the plasma edge. The magnetic field in the RFP is strongly sheared and multiple resonance surfaces exist across the minor radius at locations where the safety factor $q(r) = rB_t / RB_p$ is a rational number m/n .

In the Madison Symmetric Torus (MST) RFP (Ref. 3) (major plasma radius $R = 1.5$ m, minor radius $a = 0.52$ m) global tearing modes, excited during internal reconnection events, lead to rapid momentum transport and parallel momentum relaxation.^{4,5} This phenomenon has also been predicted analytically⁶ and observed in numerical simulations.⁷

In the framework of magnetohydrodynamics, the parallel mean-field momentum balance equation can be written as

$$\rho \frac{\partial \langle V_{\parallel} \rangle}{\partial t} = \langle \tilde{\mathbf{j}} \times \tilde{\mathbf{B}} \rangle_{\parallel} - \rho \langle (\tilde{\nabla} \cdot \nabla) \tilde{\mathbf{V}} \rangle_{\parallel}, \quad (1)$$

where \mathbf{j} , \mathbf{B} , \mathbf{V} , ρ are the current density, magnetic field, plasma velocity, and the mass density, respectively. The first term on the right hand side is the Maxwell stress and the second term is the Reynolds stress. To derive Eq. (1), we (a)

represented each plasma quantity as a sum of its mean-field value and a nonaxisymmetric fluctuating component (denoted by a tilde), (b) performed averaging over a magnetic flux surface (denoted by $\langle \cdots \rangle$), and took the component parallel to the equilibrium magnetic field. The pressure gradient term vanishes upon the flux-surface averaging and the other terms are negligibly small.

In this article, we present design of several probes developed for measuring the fluctuation-induced Maxwell and Reynolds stresses in the momentum balance equation. To determine the Maxwell stress we employ a magnetic probe, which consists of six magnetic coil triplets. The combination of a Mach probe and an optical⁸ probe allows for the measurements of the Reynolds stress.

II. MAXWELL STRESS MEASUREMENTS

The Maxwell stress term in Eq. (1) can be further simplified by (a) expressing the current density fluctuations using Ampere's law $\mu_0 \tilde{\mathbf{j}} = \nabla \times \tilde{\mathbf{B}}$ and magnetic flux conservation $\nabla \cdot \tilde{\mathbf{B}} = 0$, (b) performing the flux-surface averaging and taking into account that $\partial(\cdots)/\partial\theta$ and $\partial(\cdots)/\partial\varphi$ components of the Maxwell stress (θ -poloidal, φ -toroidal directions) vanish after the flux-surface average, and (c) utilizing the fact that the mean magnetic field is primarily in the poloidal direction near the reversal surface. As a result, the parallel component of the Maxwell stress in the cylindrical coordinates can be expressed as

$$\langle \tilde{\mathbf{j}} \times \tilde{\mathbf{B}} \rangle_{\parallel} = \frac{1}{\mu_0} \left(\frac{\partial}{\partial r} + \frac{2}{r} \right) \langle \tilde{B}_r \tilde{B}_{\theta} \rangle. \quad (2)$$

As it can be seen from Eq. (2), evaluation of the Maxwell stress requires measurements of the correlation product of two fluctuating magnetic field components at two spatial lo-

^{a)} Contributed paper, published as part of the Proceedings of the 17th Topical Conference on High-Temperature Plasma Diagnostics, Albuquerque, New Mexico, May 2008.

^{b)} Electronic mail: kuritsyn@wisc.edu.

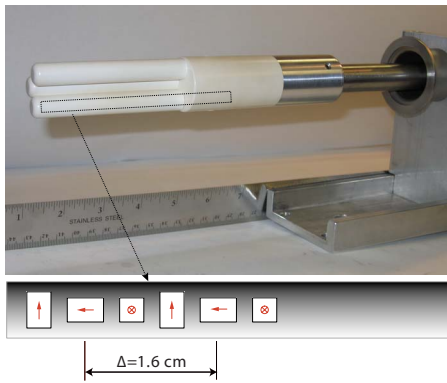


FIG. 1. (Color online) Photograph of the magnetic probe with the schematic of the coils layout in one of the legs.

cations separated radially. Such measurement has been conducted in the MST edge with an insertable array of magnetic pickup coils. The layout of the probe is shown in Fig. 1. It consists of three supporting “legs” made of boron nitride, which have machined cavities for magnetic coils and wires, mounted on a common base. Each leg has six embedded magnetic coils (two triplets). Magnetic coils are made from small ($\sim 5 \times 3 \times 3 \text{ mm}^3$) chip inductors manufactured by CoilCraft Inc. (part No. 1812CS-333XJLB) with an effective area of 9.15 cm^2 . The coils and the wires are also covered by the boron nitride powder mixed with a low expansion liquid cement (part No. 29 from Sauerisen Inc.) for additional protection. The legs are painted with silver paint for electrostatic shielding and placed inside boron nitride enclosures. The enclosures are screwed into the base and can be easily replaced if damaged by plasma, without probe disassembly. The triplets are spaced 1.6 cm in the radial direction and 1.1 cm in the poloidal and toroidal directions. The temperature of the coils, inferred by monitoring the coil resistance, was as high as $300 \text{ }^\circ\text{C}$ during the plasma shots, so the usage of solder alloy with a higher melting point is required for probe construction.

To obtain the magnetic field, the signals detected by the coils are amplified (typical gains=5–50) and integrated ($RC=0.1 \text{ ms}$) using in-house built electronics. The overall frequency response of the circuitry is $\sim 250 \text{ kHz}$, which is sufficient for accurate measurements of the tearing modes of interest, whose frequencies are typically below 50 kHz . Data were digitized at a rate of 200 kHz .

The probe was bench calibrated using a set of Helmholtz coils. In addition, the calibration was done *in situ* using the MST vacuum toroidal field. The calibration procedures included measuring and subtracting the parasitic pickup due to a slight coil misalignment.

III. REYNOLDS STRESS MEASUREMENTS

The Reynolds stress can be represented in a form similar to that of the Maxwell stress, if one assumes that plasma is incompressible, i.e., $\nabla \cdot \mathbf{V} = 0$,

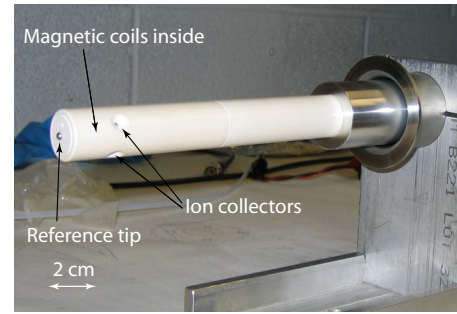


FIG. 2. (Color online) Photograph of the Mach probe.

$$\langle \tilde{\mathbf{V}} \nabla \tilde{\mathbf{V}} \rangle_{\parallel} = \left(\frac{\partial}{\partial r} + \frac{2}{r} \right) \langle \tilde{\mathbf{V}}_r \tilde{\mathbf{V}}_{\theta} \rangle. \quad (3)$$

The incompressibility assumption is valid for MST plasmas since the characteristic time scale of fluctuations of interest is larger than the characteristic length divided by the ion sound speed. To evaluate the Reynolds stress based on Eq. (3) it is sufficient to measure the velocity correlator only at one spatial location in a given discharge and then calculate the radial derivative relying on good shot-to-shot reproducibility. For compressible plasma, the spatial derivatives and flux-surface average operators do not commute and measurements become much more complicated because simultaneous flow measurements at multiple spatial points need to be performed.

To measure the fluctuation-induced Reynolds stress we have employed a combination of an insertable optical probe⁸ and a Mach probe. The probes are positioned on adjacent MST ports so that the distance between their measurement points was only few centimeters, much less than the wavelengths of the tearing mode fluctuations of interest ($\sim 1 \text{ m}$). The size of the probes ($\sim 2 \text{ cm}$) is much smaller than the wavelengths of the tearing modes so the probes are not expected to make a significant perturbation to those modes.

The optical probe, whose design is described in detail in Ref. 8, is utilized to measure the radial velocity fluctuations using Doppler spectroscopy. Light from the plasma is collected by a fiber bundle inserted into the plasma and transported to a high-resolution spectrometer. Usage of a collimator and a view dump allows for light collection locally with spatial localization of $\sim 2 \text{ cm}$. The He II 4686 \AA impurity line, whose emission was enhanced by adding helium into the discharge, was utilized in these measurements. The dispersion of the instrument at 4686 \AA is 0.235 \AA per photomultiplier tube channel. The typical signal level at $10 \mu\text{s}$ integration time is 100 photoelectrons, which according to the Poisson statistics gives a signal-to-noise ratio of 10. The resultant uncertainty for the velocity fit is estimated to be $\sim 2 \text{ km/s}$.

The poloidal and toroidal bulk plasma flows are measured by a movable Mach probe (shown in Fig. 2) consisting of four electrodes (two Mach pairs separated by 90°). The electrodes are placed inside a boron nitride enclosure (2 cm diameter). Four 2 mm tapered apertures in the enclosure determine the current collection area. The electrodes are biased negatively up to 350 V with respect to the central reference tip, which is sufficient to get to the ion current saturation

regime. In-house built electronics with a frequency response of 50 kHz is used for signal detection. The probe also has a set of five magnetic coils (a pair of B_p , B_t coils from Coil-Craft Inc. and one hand-wound B_r coil), which are used for accurate positioning of the probe with respect to the magnetic field as well as for measuring correlation between magnetic and velocity fields.

We have employed an unmagnetized model developed by Hutchinson⁹ to interpret the results, which predicts

$$V_{\text{flow}} = 0.746 \times \sqrt{\frac{T_e}{M_i}} \ln \frac{I_{\text{up}}}{I_{\text{down}}}, \quad (4)$$

where T_e is the electron temperature, M_i is the ion mass, I_{up} and I_{down} are the currents collected on the upstream and downstream sides of the probe, respectively.

For the MST Mach probe, the diameter of the electrode aperture is much smaller than the ion gyroradius, but the ratio of the ion gyroradius to the probe diameter $\rho_i/d_p \sim 0.5$, so we have used the work of Peterson *et al.*¹⁰ to estimate the degree to which magnetization effects are important. Applying the tests from Ref. 10 to the MST Mach probe verifies that ion collection can be regarded as unmagnetized.

In addition, we have compared the Mach probe measurements of the toroidal flow, induced in a controlled way by the edge biasing, to passive spectroscopic measurements using IDS-I spectrometer.¹¹ Carbon impurity emission from C III 2296.87 Å line was utilized for spectroscopy. The flow measurements obtained by the two methods are found to be in a relatively good agreement.

IV. EXAMPLE OF THE EXPERIMENTAL RESULTS

The experiments described in this article have been conducted in the MST RFP in a regime of low plasma current $I_p = 200$ kA, which allowed routine operation of the probes in the plasma edge ($0.75 \leq r/a \leq 1.0$). The other operating parameters are deuterium plasma with the line averaged density $\bar{n} = 1 \times 10^{13} \text{ cm}^{-3}$, the reversal parameter $F = -0.2$, and the pinch parameter $\theta = 1.7$.

MST plasmas exhibit quasiperiodic reconnection (relaxation) events with a period of several milliseconds. Since plasma is rotating in the laboratory frame and reconnection events occur randomly in time, measurements performed at one spatial location effectively sample the flux surface. Therefore, the flux-surface averaging in Eqs. (2) and (3) can be replaced by the conditional averaging over ensemble of similar events (see Ref. 12 for more details).

Figure 3 presents experimental data gathered near the reversal surface $B_t = 0$ at $r/a = 0.8$. The zero point on the time axis corresponds to the peak of the reconnection rate. Both the Maxwell and Reynolds stresses are individually large, but they are oppositely directed, with the difference on the order of the ion inertial term (measured by the Mach probe).

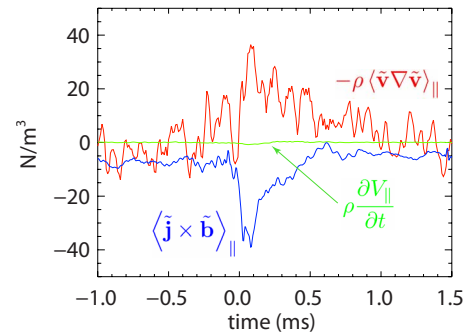


FIG. 3. (Color online) Momentum balance in the MST RFP near the reversal surface through the reconnection event. The level of rapid oscillations on the data curves for the Maxwell and Reynolds stresses indicates the experimental uncertainty.

The measurement of the Maxwell stress in the edge of MST is consistent with the measurement performed with the laser Faraday rotation diagnostic in the core, near $q = 1/6$ resonant surface.¹³ There, the Maxwell stress is observed to be much larger than the ion inertial term measured by passive spectroscopy and also inferred from the rotation of the locally resonant tearing modes.

ACKNOWLEDGMENTS

The authors would like to thank D. Ennis, S. Gan-gadhara, and R. Magee for assistance with the spectroscopic measurements, D. Craig for useful discussions, and MST engineers and technicians for excellent technical support. This work was supported by U.S. DOE and NSF.

¹K. H. Burrell, *Phys. Plasmas* **4**, 1499 (1997).

²E. J. Strait, T. S. Taylor, A. D. Turnbull, J. R. Ferron, L. L. Lao, B. Rice, O. Sauter, S. J. Thompson, and D. Wroblewski, *Phys. Rev. Lett.* **74**, 2483 (1995).

³R. N. Dexter, D. W. Kerst, T. W. Lovell, S. C. Prager, and J. C. Sprott, *Fusion Technol.* **19**, 131 (1991).

⁴A. K. Hansen, A. F. Almagri, D. Craig, D. J. Den Hartog, C. C. Hegna, S. C. Prager, and J. S. Sarff, *Phys. Rev. Lett.* **85**, 3408 (2000).

⁵G. Fiksel, A. F. Almagri, J. K. Anderson, T. M. Biewer, A. P. Blair, D. L. Brower, B. E. Chapman, D. Craig, D. J. Den Hartog, W. X. Ding, C. B. Forest, C. C. Hegna, R. Gatto, J. Goetz, K. J. McCollam, V. V. Mirnov, R. O'Connell, S. C. Prager, J. C. Reardon, J. S. Sarff, P. W. Terry, S. D. Terry, and MST Team, Proceedings of 19th IAEA Fusion Energy Conference, 2002, p. EX/P4, 01.

⁶C. C. Hegna, *Phys. Plasmas* **5**, 2257 (1998).

⁷F. Ebrahimi, V. V. Mirnov, S. C. Prager, and C. R. Sovinec, *Phys. Rev. Lett.* **99**, 075003 (2007).

⁸A. Kuritsyn, D. Craig, G. Fiksel, M. Miller, D. Cylinder, and M. Yamada, *Rev. Sci. Instrum.* **77**, 10F112 (2006).

⁹I. H. Hutchinson, *Plasma Phys. Controlled Fusion* **44**, 1953 (2002).

¹⁰B. J. Peterson, J. N. Talmadge, D. T. Anderson, F. S. B. Anderson, and J. L. Shohet, *Rev. Sci. Instrum.* **65**, 2599 (1994).

¹¹D. J. Den Hartog and R. J. Fonck, *Rev. Sci. Instrum.* **65**, 3238 (1994).

¹²A. Kuritsyn, G. Fiksel, A. F. Almagri, S. C. Prager, J. S. Sarff, and T. D. Tharp, Proceedings of the IEEE PPPS Conference, Albuquerque, NM, 2007, p. 20.

¹³W. X. Ding, D. L. Brower, B. H. Deng, D. Craig, S. C. Prager, and V. Svidzinski, *Rev. Sci. Instrum.* **75**, 3387 (2004).